AD-A050 473 ROCKWELL INTERNATIONAL THOUSAND OAKS CALIF SCIENCE --ETC F/G 11/6
MECHANICAL BEHAVIOR OF TITANIUM ALLOYS (FORMATION BEHAVIOR OF A--ETC(U)
JAN 78 C G RHODES, N E PATON N00014-76-C-0598

UNCLASSIFIED SC5056-1TR NL

| OF |
AD A050473

END
DATE FILMED
3-78
DDC

(12)
B.S.

SC5056.1TR

COPY NO. 26

MECHANICAL BEHAVIOR OF TITANIUM ALLOYS

TECHNICAL REPORT

Submitted to:

Office of Naval Research

by

C. G. Rhodes and N. E. Paton

Approved for Public Release; Distribution Unlimited

Rockwell International
Science Center

UNCLASSIFIED

SECURITY CLASSIFICATION OF THIS PAGE (When Data Entered)

REPORT DOCUMENTATION PAGE	READ INSTRUCTIONS BEFORE COMPLETING FORM
1. REPORT NUMBER (6)	2. GOVT ACCESSION NO.
3. RECIPIENT'S CATALOG NUMBER (9)	
4. TITLE (and Subtitle) MECHANICAL BEHAVIOR OF TITANIUM ALLOYS (FORMATION BEHAVIOR OF α/β INTERFACE PHASE IN Ti-6Al-4V). alpha/beta	5. TYPE OF REPORT & PERIOD COVERED TECHNICAL REPORT. FEB [redacted] 76 - FEB [redacted] 77.
(14)	6. PERFORMING ORG. REPORT NUMBER SC5056-1TR
7. AUTHOR(s) (10) C. G./RHODES [redacted] N. E./PATON	8. CONTRACT OR GRANT NUMBER(s) (15) N0014-76-C-0598 New
9. PERFORMING ORGANIZATION NAME AND ADDRESS SCIENCE CENTER, ROCKWELL INTERNATIONAL 1049 CAMINO DOS RIOS THOUSAND OAKS, CA 91360	10. PROGRAM ELEMENT, PROJECT, TASK AREA & WORK UNIT NUMBERS 471
11. CONTROLLING OFFICE NAME AND ADDRESS DR. BRUCE MAC DONALD OFFICE OF NAVAL RESEARCH 800 N. QUINCY, ARLINGTON, VA 22217	12. REPORT DATE (11) JANUARY 13, 1978 13 Jan 78
	13. NUMBER OF PAGES (12) 29 32p.
14. MONITORING AGENCY NAME & ADDRESS(if different from Controlling Office)	15. SECURITY CLASS. (of this report) UNCLASSIFIED
	15a. DECLASSIFICATION/DOWNGRADING SCHEDULE

16. DISTRIBUTION STATEMENT (of this Report)

APPROVED FOR PUBLIC RELEASE, DISTRIBUTION UNLIMITED

DDC RECEIVED FEB 27 1978 B

17. DISTRIBUTION STATEMENT (of the abstract entered in Block 20, if different from Report)

18. SUPPLEMENTARY NOTES

19. KEY WORDS (Continue on reverse side if necessary and identify by block number)

Titanium, Electron Microscopy, Interface Phase

20. ABSTRACT (Continue on reverse side if necessary and identify by block number)

The conditions for formation of the interface phase, or interfacial layer, in Ti-6Al-4V have been studied systematically. The interface phase does not grow during isothermal treatments, but rather only during cooling from elevated temperatures to about 650°C. The width of the interfacial layer is a function of the cooling rate, having a maximum of about 4000Å at 28°C/hr. The interface phase forms initially with an fcc structure which subsequently transforms to hcp α phase. A theoretical description of the mechanisms of interface phase formation is presented.

DD FORM 1 JAN 73 1473 EDITION OF 1 NOV 65 IS OBSOLETE

UNCLASSIFIED

SECURITY CLASSIFICATION OF THIS PAGE (When Data Entered)

389 949

Rockwell International
Science Center

SC5056.1TR

MECHANICAL BEHAVIOR OF TITANIUM ALLOYS

(FORMATION BEHAVIOR OF α/β INTERFACE PHASE IN Ti-6Al-4V)

FEBRUARY 1976 to FEBRUARY 1977

Submitted to:

Dr. Bruce MacDonald
Office of Naval Research

by

C. G. Rhodes and N. E. Paton

13 JANUARY 1978

Rockwell International
Science Center
SC5056.1TR

FORMATION CHARACTERISTICS OF THE α/β INTERFACE PHASE IN Ti-6Al-4V

C. G. Rhodes and N. E. Paton
Science Center, Rockwell International
Thousand Oaks, California

ABSTRACT

The conditions for formation of the interface phase, or interfacial layer, in Ti-6Al-4V have been studied systematically. The interface phase does not grow during isothermal treatments, but rather grows only during cooling from elevated temperatures to about 650°C. The width of the interfacial layer is a function of the cooling rate, having a maximum of about 4000Å at 28°C/hr. The interface phase forms initially with an fcc structure which susbsequently transforms to hcp α phase. A theoretical description of the mechanisms of interface phase formation is presented.

The microstructural feature which occurs under certain conditions at the interphase boundaries of alpha and beta phases in titanium alloys has been called alternatively "interface phase"[1] or "interfacial layer."[2] This feature is most easily studied by transmission electron microscopy because it grows to a maximum width of about one micron and generally is considerably less than that. The role of interface phase in the $\beta \rightleftharpoons \alpha$ phase transformation and its potential effect on mechanical properties are two areas which warrant further study.

The α/β boundaries have been shown to be an important factor in the fracture of two-phase titanium alloys in the cases of tensile[3] and fatigue[4] testing. The presence of an interfacial layer may influence the fracture process by providing an easy crack path or by providing crack initiation sites. Strength and ductility may be affected if the presence of the interface phase inhibits the transfer of slip between the α and β phases. Margolin et al.[5], on the other hand, have recently suggested that interface phase would have only minor effects on mechanical properties.

Previous work[1,2] indicated that the interfacial layer could form either with an fcc structure or with an hcp structure, and evidence was presented that the interface phase was α phase in a "non-Burgers" orientation[1] or in a Burgers orientation different from that of the adjacent primary α.[5] A study was undertaken to establish systematically the conditions for interface phase formation, its crystallography, its

stability, and its effect on tensile properties in Ti-6Al-4V. This paper reports the results of the formation kinetics and crystallography portions of the study.

EXPERIMENTAL

Two heats of Ti-6Al-4V were used in this work, the chemical analyses are listed in Table I. The "as-received" microstructure of both heats consisted of ~90% equiaxed primary alpha particles, having approximately a 12 μm diameter in a continuous β matrix. The heat treatments were carried out with the samples either in a dynamic inert gas atmosphere or encapsulated in evacuated ampoules. The isothermal reaction treatments were accomplished by quenching samples directly from an inert-atmosphere furnace held above the beta transus into a fluidized bed held at the reaction temperature. A programmable controller supplying power to the furnace was used for controlled-cooling-rate treatments.

Tensile tests were conducted on an Instron testing machine with an extensometer attached to the sample. The samples were in the form of round bars with a 6.35 mm diameter and 31.75 mm gauge length. A strain rate of 2.6×10^{-4} sec^{-1} was used in all tensile tests.

Thin foils for transmission electron microscopy were prepared by conventional electropolishing techniques[6] or by ion milling.[7] The foils were examined in a Philips EM-300 electron microscope equiped with a double tilt goniometer stage.

Since the projected width of the interfacial layer in an electron micrograph is dependent upon the angle which the interface makes with the electron beam, a standard geometric-crystallographic condition was established for all interface phase measurements. This condition calls for the interface to be parallel to the electron beam within 5^{o} and for the α phase to be in a two-beam diffracting condition with g = 0002. The standard condition can be achieved in the following manner. When 6-4 is cooled from above the beta transus, the alpha phase which results from the $\beta \rightarrow \beta + \alpha$ transformation forms as elongated plates. The rate of cooling generally controls the aspect ratio of the plates. Previous work[8,9] has shown that these nucleation-and-growth plates have a {334} β habit plane which corresponds through the Burgers relation to a $\{41\bar{5}0\}$ α phase plane[8] and is identical to the martensite habit plane.[10] The plates grow with the long direction of the plate parallel to [0001] α and [011] β. The {4150} α habit plane lies 11^{o} from $\{10\bar{1}0\}$ α about the [0001] α. The standard condition for electron microscope observations can then be achieved by a 15^{o} tilt about the [0001] α from the $<10\bar{1}0>$ α zone; the standard condition lies halfway between the <1010> and <1120> α zones.

RESULTS

I. Layer Formation Behavior

The interfacial layer has been shown previously[1,2] to occur either with a dense internal structure (called a striated layer) or with no internal structure (called a monolithic layer). The striated layer was interpreted as

having the hcp structure of the alpha phase, but in a different orientation from the adjacent primary alpha. The monolithic layer was shown to have an fcc structure.

In order to establish the conditions under which the interface phase will grow, two heat treat schedules were devised. The first was a series of isothermal reaction treatments aimed at establishing a T-T-T diagram for interface phase growth. Samples of 6-4 were solutionized above the beta transus (at 1030°C) and then quenched directly to one of several temperatures below the β transus. The samples were held at the reaction temperature for times from 1 minute to 24 hours. Electron microscopy of the samples revealed that there was no growth of the interface phase during isothermal treatments. For example, Figure 1 shows the alloy held for 2 minutes (a) and 24 hours (b) at 704°C (1300°F). The 704°C (1300°F) reaction temperature is above the martensite start temperature (Ms) for Ti-6Al-4V[11] and the beta to alpha transformation, which is approximately 25% complete after 2 minutes, is complete after about 4 hours. Isothermally reacting below the Ms does not alter the observed result of negligible layer growth during isothermal treatment, as illustrated in Figure 2. In all cases the layer was so narrow that the nature of the layer (striated or monolithic) could not be determined either by selected area diffraction (SAD) or by imaging.

The second heat treat schedule was a series of controlled cooling treatments in two parts: cooling from above the β transus and cooling from below the β transus. The samples were cooled to temperatures in the range of 472°C (800°F) to 927°C (1700°F) at rates ranging from 2.8°C/hr

(5^{o}F/hr) to 555^{o}C/hr (1000^{o}F/hr) and were water quenched immediately upon reaching the lower temperature. Samples were also cooled to room temperature. These treatments produced interfacial layers of varying thicknesses. The widths of the layers were measured for all of the treatments and the results obtained from the samples cooled from above the β transus are presented in Figure 3. Samples cooled to temperatures below 760^{o}C (1400^{o}F) appear to fall on a single curve which shows a maximum layer width at 28^{o}C/hr (50^{o}F/hr). The samples cooled to 760^{o}C (1400^{o}F) exhibit a narrower layer width than those cooled further, and also appear to have a maximum around 28^{o}C/hr (50^{o}F/hr). Samples cooled to 816^{o}C (1500^{o}F) and above had no interfacial layer in the α-β interfaces.

The interface phase was predominantly the striated type in all cases. Although the monolithic type layer could be observed in most samples, it rarely, if ever, was present in more than 50% of the interfacial area, and more generally was observed in 25% or less of the interfaces. No systematic correlation of the amount of monolithic interface phase with cooling rate or lower temperature could be discerned. The monolithic layer was generally on the order of one-half the width of the striated layer in any one sample. The values in Figure 3 are the mean values of measurements of both striated and monolithic layers and the fairly large error bars (which are 95% confidence intervals) reflect the large difference in widths of the two types of layers. Examples of the interface phase in these samples are shown in Figures 4 and 5. Those layers in samples cooled to 649^{o}C (1200^{o}F), Figure 4, have a well-developed striated structure, while those in samples cooled to 760^{o}C (1400^{o}F), Figure 5, have a less developed internal structure.

A series of samples was controlled cooled from below the β transus. These samples were cooled from an upper temperature of 982°C (1800°F), 927°C (1700°F) or 871°C (1600°F) at rates of 28°C/hr (50°F/hr), 56°C/hr (100°F/hr) and 112°C/hr (200°F/hr). As was the case for samples cooled from above the β transus, no interface phase was formed on cooling to 816°C (1500°F) and higher. Those cooled to 760°C (1400°F) and lower showed mainly striated layers similar to the results observed for samples cooled from above the β transus.

II. Crystallography of Interfacial Layer

The monolithic layer has an fcc structure, as reported previously,[1,2] with a lattice parameter approximately 4.26A. Figure 6 is a sequence illustrating the fcc monolithic layer. The orientation relation between the fcc monolithic layer and the bcc beta phase is (110) β ||$(1\bar{1}1)$ fcc and $[\bar{1}11]$ β ||[110] fcc, which is the Kurdjumov-Sachs relationship. The orientation relation between the fcc monolithic layer and the hcp alpha phase is (0002)α ||$(1\bar{1}1)$ fcc and $[11\bar{2}0]\alpha$ || [110] fcc. This relationship has close packed planes parallel, and close packed directions parallel in the two phases.

Occasionally, a monolithic layer can be found with a few internal striations such as shown in Figure 7. Trace analysis of these striations reveals that they lie in a (111) plane, which is the twinning plane in fcc structures, suggesting that these features may be twins or stacking faults, which also lie on (111) planes.

A striated layer is composed of a densely packed series of planar features which appear to be extending into the alpha phase, Figure 8. Trace analysis of the striations shows that they lie parallel to the basal plane of the alpha phase. The SAD pattern from a striated layer such as that in Figure 8 is composed of arced reflections as illustrated in Figure 9. This pattern is similar to that observed for Type 2 alpha[9] but in this case can be indexed as fcc with both twinned and untwinned zones present. Figure 9 illustrates the relationship $[111]\beta \,||\, [11\bar{2}0]\alpha \,||\, [110]$ fcc. To confirm this relationship and that the striated layer is mainly composed of twinned and untwinned fcc structure, Figure 10 shows another orientation of the α and β phases. In Figure 10, the β zone normal is $\bar{[}100]$ and, in agreement with the Burgers relation, the adjacent α phase is near a $[11\bar{2}0]$ zone normal.

The interface orientation for plate-shaped alpha phase was confirmed to be $\{334\}\,\beta \,||\{41\bar{5}0\}\alpha$. Additionally, several interfaces in samples having equiaxed alpha particles were analyzed. It was found that many of the noncurved interfaces had the same orientation as that observed for the plate-shaped α, namely $\{334\}\beta \,||\, \{41\bar{5}0\}\alpha$. The other most common, but far fewer than the previous, interface orientation was $\{10\bar{1}2\}\alpha$. The orientations held whether the interface phase was monolithic or striated.

DISCUSSION

The results have shown that the interfacial layer forms only during a continuous change in temperature and is not formed by isothermal treatments. This would indicate that the interface phase is a consequence of composition

shifts and/or volumetric constraints which occur during the change in relative amounts of alpha and beta phases present. During slow cooling, there is a continuous increase in the equilibrium volume fraction of α phase and a corresponding decrease in volume fraction of β phase which occurs principally as growth of the primary α particles rather than nucleation of new α particles. Since the equilibrium α phase in 6-4 contains $<1.2\%$ vanadium,[12] there is continual diffusion of vanadium from the newly formed α into the β phase as the α-β interface advances into the β phase. The composition gradient thus established may influence the formation of interface phase as described later.

The observations that the monolithic (fcc) layer exists in 50% or less of the interface area and always in conjunction with the striated form suggests that the monolithic is a transient form of the interface phase. Figure 11 illustrates that the fcc layer is frequently observed adjacent to the beta but in combination with the striated interface phase which in turn is adjacent to the growing primary α particle. The fact that growth is taking place into the beta suggests that the monolithic fcc phase forms first, as a nonequilibrium transition phase. Another point which would appear to support the view that monolithic is a transient form is that the fcc layer occurs most frequently on curved boundaries convex into the beta phase. Since boundary curvature might be expected to be a measure of the driving force for boundary motion, this suggests that the most rapidly moving boundaries (those farthest from chemical equilibrium) are the ones with the most monolithic fcc interface phase. On the other hand, straight boundaries were found to be frequently associated with the striated interface phase, as might be expected if these were closer to equilibrium.

We believe that the bcc β phase transforms initially to an fcc structure as a result of the composition gradients described above. As reported earlier,[2] the fcc structure is an intermediate atomic arrangement in the β→α transformation. Calculations show that the expected lattice parameter of the fcc structure would be 1.4 times that of the β phase. The lattice parameter which we observe for the monolithic layer is 4.26A, which is approximately 1.3 larger than the β parameter. The high vanadium content apparently influences the β→α transformation such that the fcc transition structure is stabilized.

The transition from fcc interface phase to the striated form was, as noted earlier, frequently associated with {111} twin formation in the fcc structure. That is, the initial form of interface phase is a narrow fcc monolithic layer which is subsequently modified by the formation of (111) twins. The resulting structure with a high density of these features then transforms to equilibrium hcp alpha phase resulting in thin plates of alpha phase. Inspection of the crystallography of the fcc to hcp transformation reveals that both the twinned and untwinned plates will transform to an identical alpha phase orientation, which is the Burgers orientation. Thus the primary alpha particle grows during cooling with its original orientation in spite of the complex transformation sequence. The newly formed α phase plates in the interface region appear to retain a high density of the prior fcc dislocations, while the twin boundaries seem to persist as internal boundaries in the α phase. Although most of this debris appears to eventually anneal out, many basal plane "faults" are present in the primary alpha particles and are probably remnants of the fcc twin boundaries, Figure 12.

This representation of interface phase formation precludes the presence of Type 2 alpha.[9] The SAD patterns from interface phase had previously[1,2] been compared to those arising from Type 2 α and their similarity led to the conclusion that the striated interface phase was hcp α phase of an orientation different from the adjacent alpha. However, this work shows that the interface phase patterns are, in fact, from twinned fcc structures. It is not surprising that twinned fcc and twinned hcp (Type 2 α) having the (110) $||$ $(11\bar{2}0)$ and [111] $||$ [0001] relationship (with d-spacings of parallel planes within 5%) would generate similar diffraction patterns with respect to the parent β phase.

In order for the above description of interface phase formation to be acceptable, the possible driving forces involved in the reactions should be examined. The metastable condition which exists during cooling was described earlier. As the α/β interface advances into the β phase, the β phase becomes more enriched in V and more vanadium must be rejected by newly formed α phase. A potential chemical driving force for the formation of interface phase results from the nonequilibrium, high vanadium content of the α/β interface region.

The influence of diffusion of vanadium and aluminum in the vicinity of the interface is difficult to assess quantitatively under these conditions where the interface is moving, the temperature is changing constantly, and the equilibrium volume fractions and compositions of the two phases are changing. However, a qualitative description of the composition and composition profile in the vicinity of the interface can be made. This has been done schematically in Figure 13. In Region I, which corresponds to the very slow

cooling rates in Figure 3, equilibrium conditions obtain producing the sharp composition gradient depicted in the figure. This holds because the $\beta \rightarrow \alpha$ transformation will be slow, allowing vanadium to diffuse from the interface into the β phase. In Region III, which corresponds to the very fast cooling rates in Figure 3, a sharp composition gradient develops because the $\beta \rightarrow \alpha$ transformation is rapid. In this case, the α phase forms with a maximum (critical) vanadium content, which is higher than the equilibrium content, because the rapid cooling rate inhibits vanadium diffusion. Region II, which corresponds to the mid-region of Figure 3, exhibits a broad composition gradient in the α/β interface region. If vanadium diffusion is slightly slower than beta transformation, the composition gradient will develop as depicted in the figure. The fcc layer will exist at the β phase side of the interface corresponding to a high vanadium content, while the hcp layer forms on the α phase side of the interface corresponding to a lower vanadium content.

In addition to the chemical change during cooling noted above, there is approximately a 5% volume expansion coincident with the $\beta \rightarrow \alpha$ transformation. This expansion, together with the larger coefficient of thermal expansion of the β phase, will place the alpha phase in a state of hydrostatic compression. Since the β phase in Ti-6Al-4V has a higher yield strength than the α phase,[13] the hydrostatic compression may be relieved by deformation the vicinity of the α/β interface where the stresses will be highest. The twins observed in the monolithic fcc layer can provide the necessary stress relief. These stresses thus account for the deformation of the monolithic layer and provide a mechanical driving force for the completion of the bcc to hcp transformation.

This model of interface phase formation predicts that the initial product of the β phase decomposition will be an fcc phase having a vanadium content higher than that of the equilibrium α phase. With continued cooling, as the monolithic (fcc) layer enlarges, the hydrostatic compressive stresses on the α phase are relieved by deformation of the fcc layer. The subsequent diffusion of vanadium from the twinned fcc layer allows it to complete the transformation to hcp alpha phase. The process continues during cooling, thus producing broad striated layers.

A final comment regarding the similarities and differences of Type 2 α[9] and interface phase seems appropriate. Type 2 α is generally observed in the isothermal decomposition of metastable β phase alloys, which are characterized by lower volume fractions of α phase (compared to α+β alloys). Since the fcc structure does not form to any significant degree during isothermal treatments, the alpha phase particles form with the hcp structure in the metastable β phase alloys. Thus the original alternatives[9] of nucleation and growth or mechanical twinning (which was subsequently supported by Margolin et al.[5]) mechanisms are not negated by the observation of fcc structures in nonisothermal transformations.

CONCLUSIONS

1. The α/β interface phase does not grow during isothermal treatments.
2. The interphase phase grows during slow cooling and its final thickness is a function of cooling rate.

3. The monolithic morphology of interface phase has a face centered cubic structure and obeys the crystallographic relationship:
   $(110)\beta \parallel (111)$ fcc $\parallel (0002)\alpha$ and $[111]\beta \parallel [110]$ fcc $\parallel [11\bar{2}0]\alpha$.
4. The fcc monolithic interface phase may be a transition structure in the $\beta \rightarrow \alpha$ transformation.
5. The interface phase may result from sluggish beta stabilizer (vanadium) diffusion away from the transforming ($\beta \rightarrow \alpha$) interface region.

ACKNOWLEDGEMENTS

We are pleased to acknowledge the assistance of R. A. Spurling, P. O. Sauers, and E. H. Wright. This work was supported by the Office of Naval Research (Contract N00014-71-C-0363).

REFERENCES

1. C. G. Rhodes and J. C. Williams, Met. Trans., Vol. 6A, 1975, pp 1670-71
2. C. G. Rhodes and N. E. Paton, Proceedings of 3rd Intern. Conf. on Ti, Moscow, 1976, in press
3. J. C. Chesnutt and J. C. Williams, Scanning Electron Microscopy/1974 (Part IV), p 895, ITT Research Institute, Chicago, 1974
4. C. A. Stubbington and A. W. Bowen, J. Mater. Sci., Vol. 9, 1974, pp 941-47
5. H. Margolin, E. Levine, and M. Young, Met. Trans., Vol. 8A, 1977, pp 373-77
6. R. A. Spurling, Met. Trans., Vol. 6A, 1975, pp 1660-61
7. R. A. Spurling, C. G. Rhodes, and J. C. Williams, Met. Trans., Vol 5, 1974, pp 2597-600
8. G. Hahn, Senior Thesis, New York Univ., cited by P. A. Albert, Trans. TMS-AIME, Vol. 197, 1953, pp 1449-50
9. C. G. Rhodes and J. C. Williams, Met. Trans., Vol. 6A, 1975, pp 2103-14
10. D. J. Maykuth, F. C. Holden, D. N. Williams, H. R. Ogden, and R. I. Jaffee, DMIC Report 136B, Battelle Memorial Institute, Columbus, Ohio, May 1961
11. L. E. Tanner, DMIC Report 46G, Battelle Memorial Institute, Columbus, Ohio, Oct. 1959
12. F. A. Shunk: Constitution of Binary Alloys, Second Supplement, p 703 McGraw-Hill Book Co., New York, 1969
13. N. E. Paton, Science Center, Rockwell International, Thousand Oaks, California, unpublished research, 1977

TABLE I

COMPOSITION BY WEIGHT OF Ti-6Al-4V

Heat	Ti	Al	V	Fe	C	O	H	N
#1	Bal	6.15	4.09	0.18	0.011	0.129	0.0067	0.019
#2	Bal	6.1	4.0	0.19	0.02	0.122	0.0088	0.018

FIGURE CAPTIONS

Fig. 1 TEM of Ti-6Al-4V isothermally reacted at 704°C (1300°F) for (a) 1 minute, (b) 24 hours.

Fig. 2 TEM of Ti-6Al-4V isothermally reacted at 593°C (1100°F) for (a) 2 minutes, (b) 24 hours.

Fig. 3 Interfacial layer width as a function of cooling rate from 1030°C (1885°F) in Ti-6Al-4V.

Fig. 4 TEM of Ti-6Al-4V cooled 28°C/hr (50°F/hr) from 1030°C (1885°F) to 649°C (1200°F) and water quenched.

Fig. 5 TEM of Ti-6Al-4V cooled 28°C/hr (50°F/hr) from 1030°C (1885°F) to 760°C (1400°F) and water quenched.

Fig. 6 TEM of Ti-6Al-4V illustrating fcc structure of monolithic interface phase: (a) SAD of interface phase in [011] fcc orientation and adjacent beta phase in [001] orientation, (b) dark field image of beta phase, (c) dark field image of interfacial layer, (d) dark field of interfacial layer.

Fig. 7 TEM of Ti-6Al-4V illustrating internal striations in monolithic layer.

Fig. 8 TEM of Ti-6Al-4V illustrating detailed structure of striated interfacial layer: (a) bright field, (b) dark field.

Fig. 9 Selected area electron diffraction pattern from striated interfacial layer.

Fig. 10 Selected area electron diffraction patterns confirming orientation relation among beta phase, interface phase, and alpha phase.

Fig. 11 TEM of Ti-6Al-4V illustrating monolithic (white) and striated (dark) interfacial layers in α/β boundary.

Fig. 12 TEM of Ti-6Al-4V demonstrating basal plane faults in primary alpha phase.

Fig. 13 Schematic description of vanadium concentration gradient in three regions of Figure 3 corresponding to (I) very slow cooling rate, (II) intermediate cooling rate, and (III) rapid cooling rate.

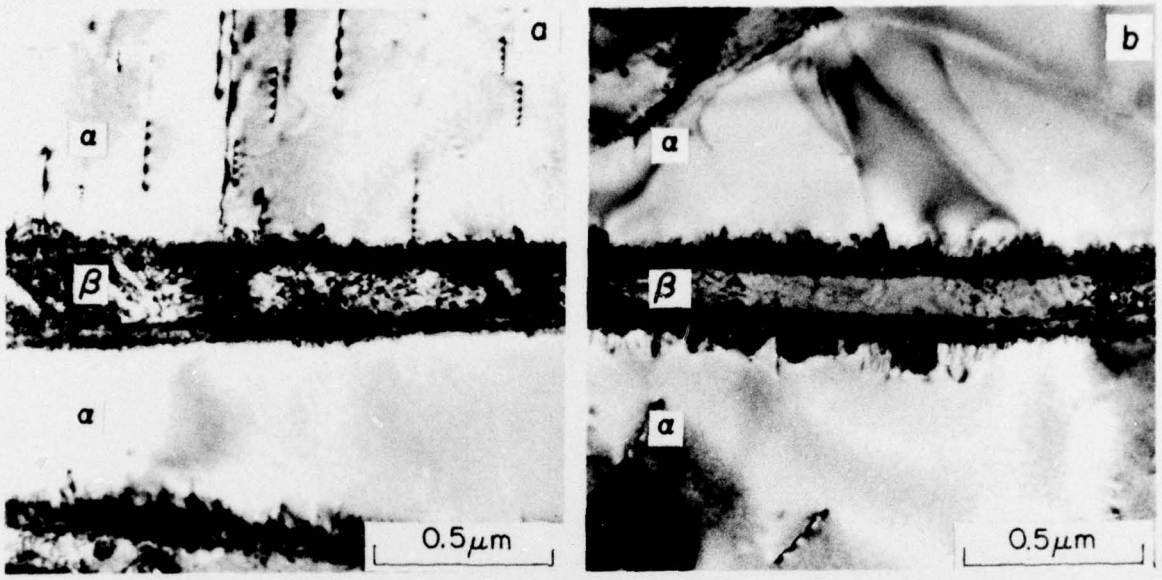

Fig. 1 TEM of Ti-6Al-4V isothermally reacted at 704°C (1300°F) for (a) 1 minute, (b) 24 hours.

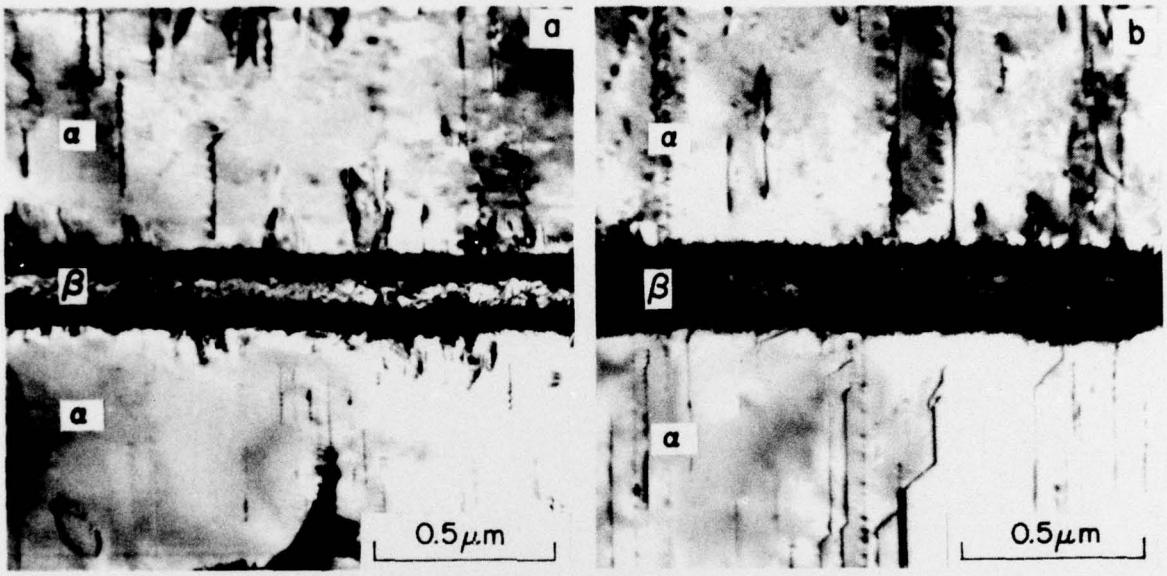

Fig. 2 TEM of Ti-6Al-4V isothermally reacted at 593°C (1100°F) for (a) 2 minutes, (b) 24 hours.

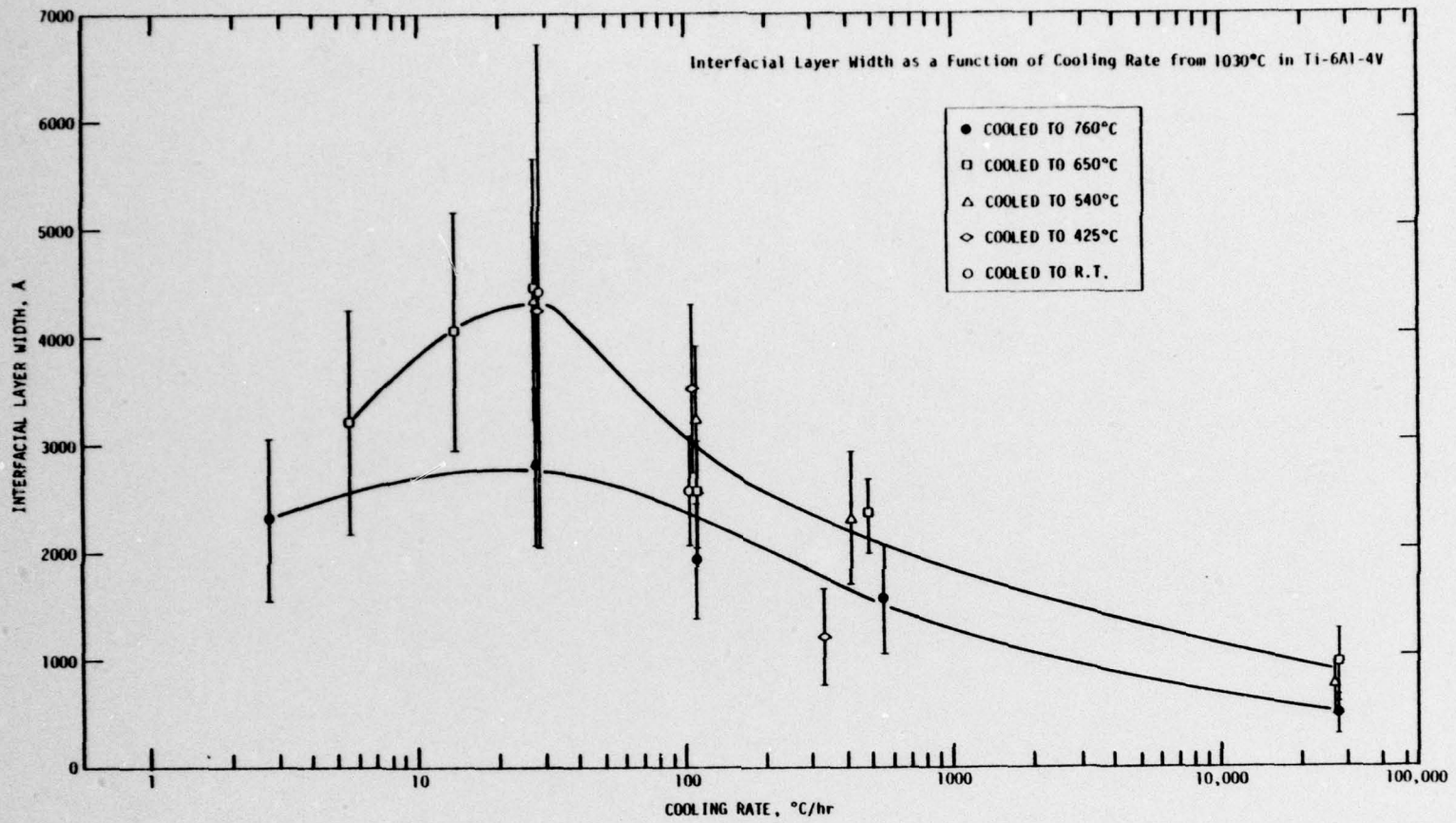

Fig. 3 Interfacial layer width as a function of cooling rate from 1030°C (1885°F) in Ti-6Al-4V.

Rockwell International
Science Center

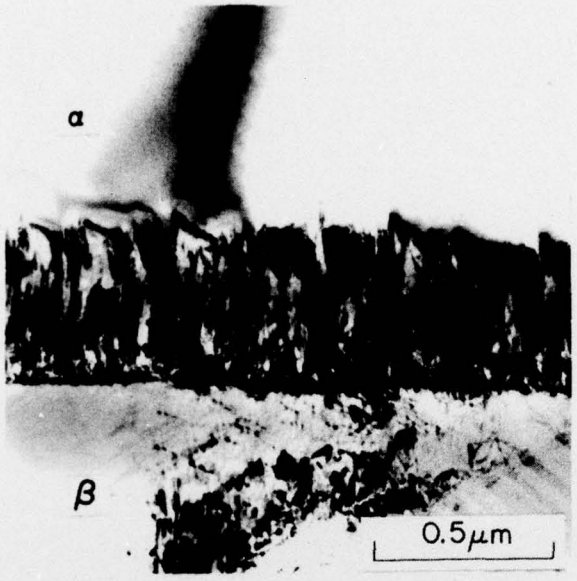

Fig. 4 TEM of Ti-6Al-4V cooled 28°C/hr (50°F/hr) from 1030°C (1885°F) to 649°C (1200°F) and water quenched.

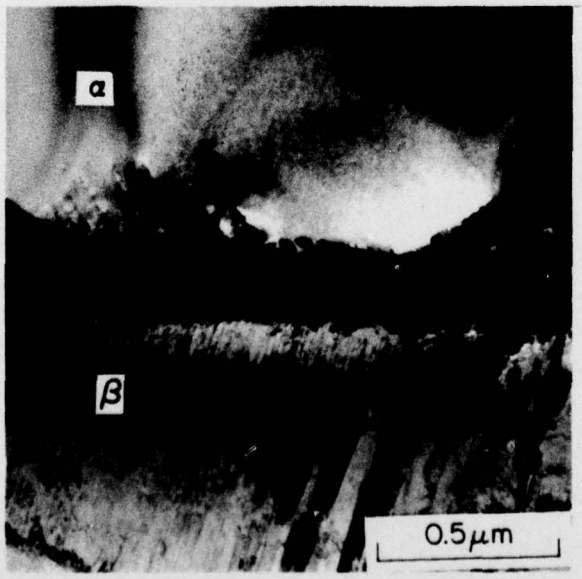

Fig. 5 TEM of Ti-6Al-4V cooled 28°C/hr (50°F/hr) from 1030°C (1885°F) to 760°C (1400°F) and water quenched.

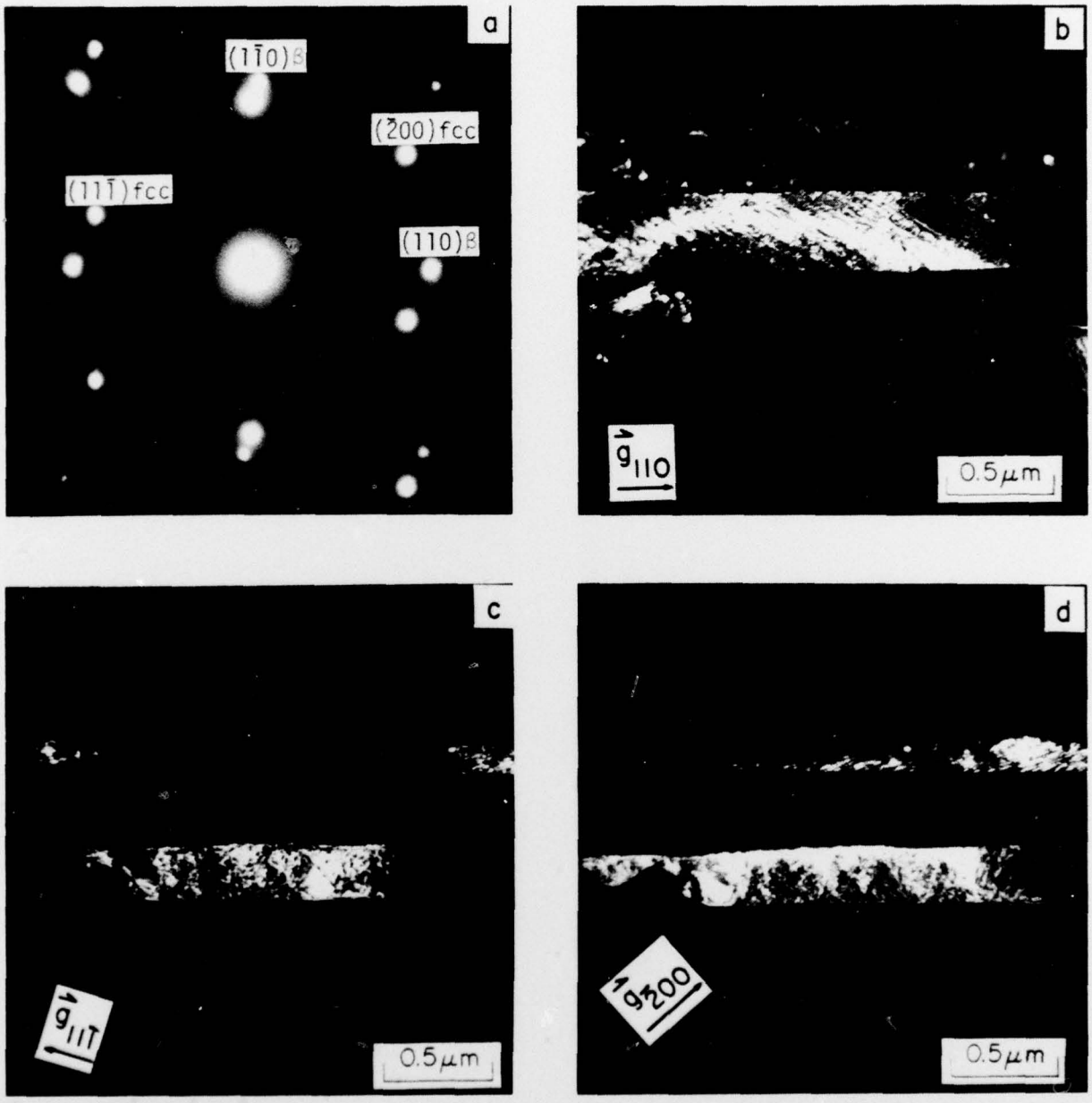

Fig. 6 TEM of Ti-6Al-4V illustrating fcc structure of monolithic interface phase: (a) SAD of interface phase in [011] fcc orientation and adjacent beta phase in [001] orientation, (b) dark field image of beta phase, (c) dark field image of interfacial layer, (d) dark field of interfacial layer.

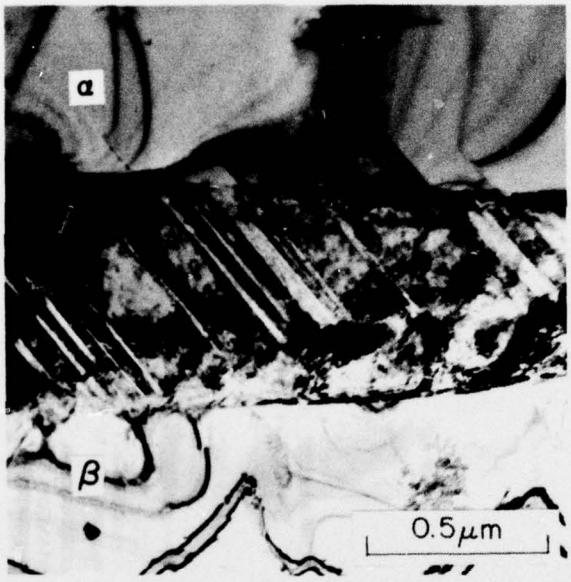

Fig. 7 TEM of Ti-6Al-4V illustrating internal striations in monolithic layer.

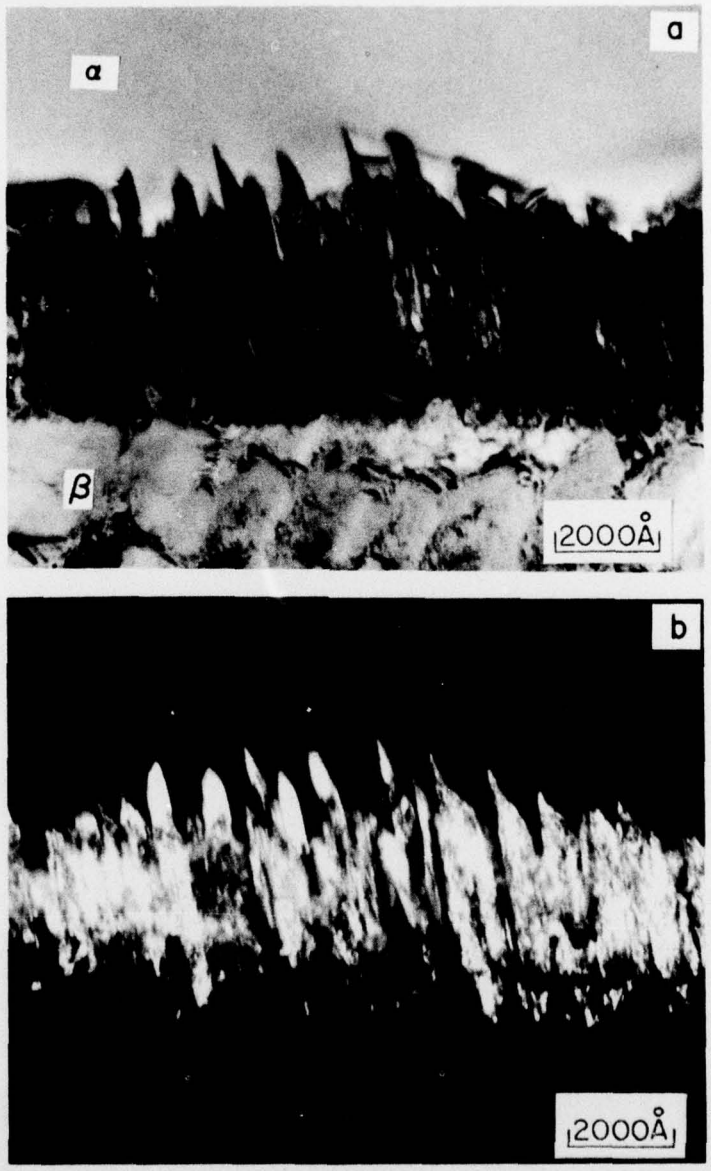

Fig. 8 TEM of Ti-6Al-4V illustrating detailed structure of striated interfacial layer: (a) bright field, (b) dark field.

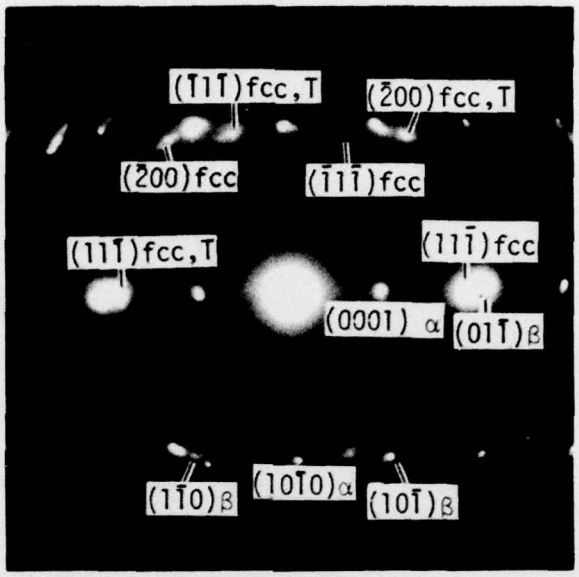

Fig. 9 Selected area electron diffraction pattern from striated interfacial layer.

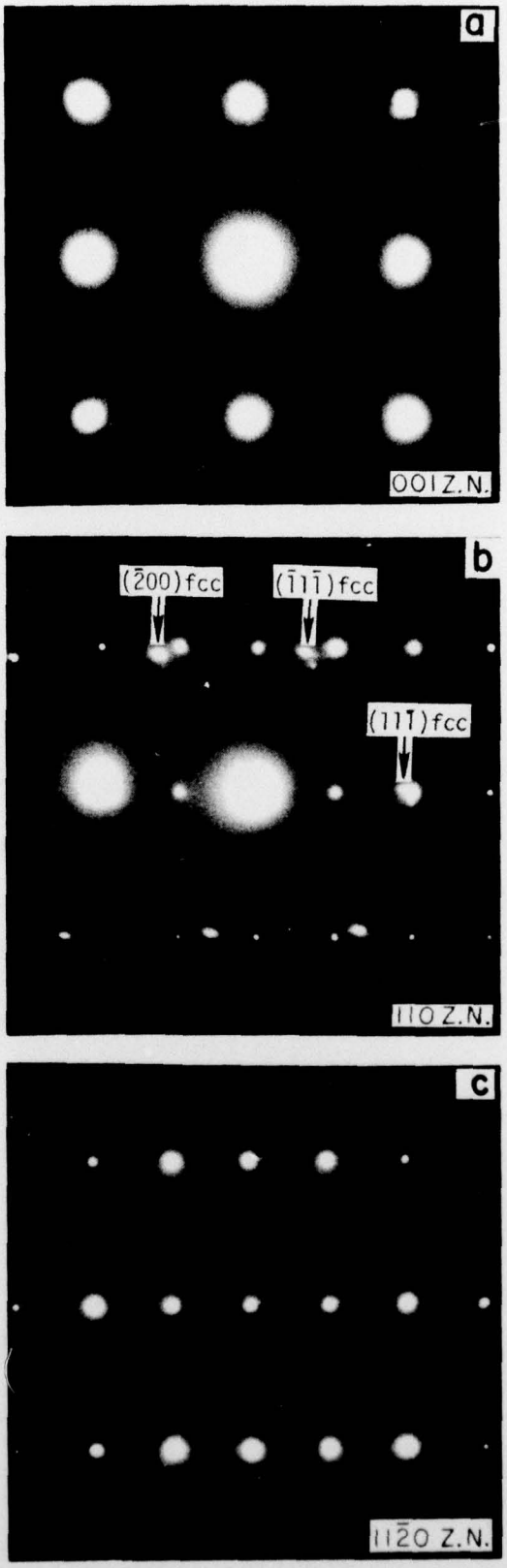

Fig. 10 Selected area electron diffraction patterns confirming orientation relation among beta phase, interface phase, and alpha phase.

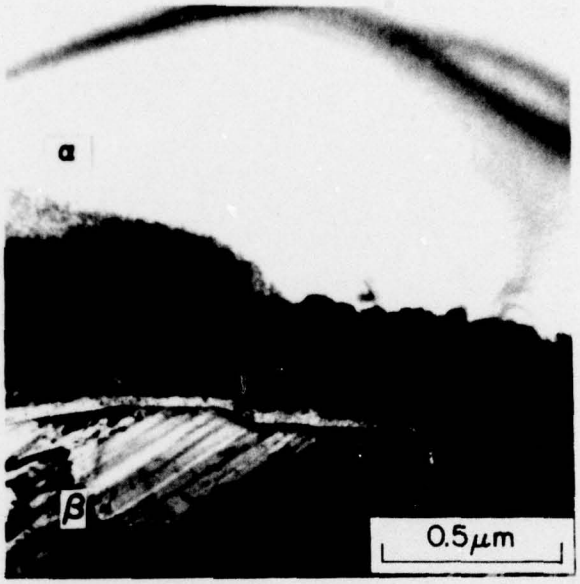

Fig. 11 TEM of Ti-6Al-4V illustrating monolithic (white) and striated (dark) interfacial layers in α/β boundary.

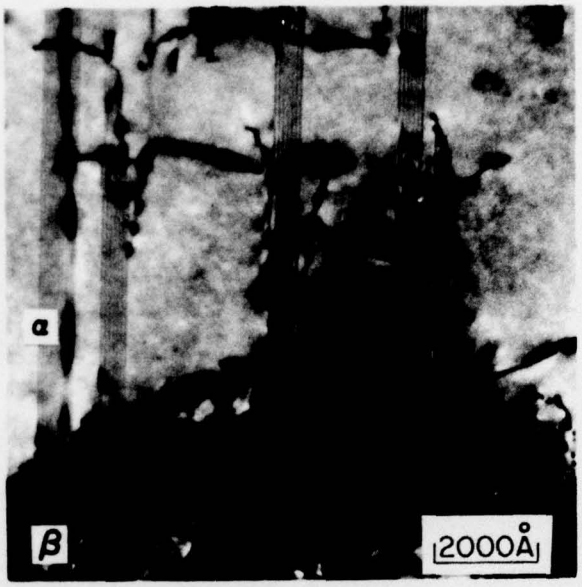

Fig. 12 TEM of Ti-6Al-4V demonstrating basal plane faults in primary alpha phase.

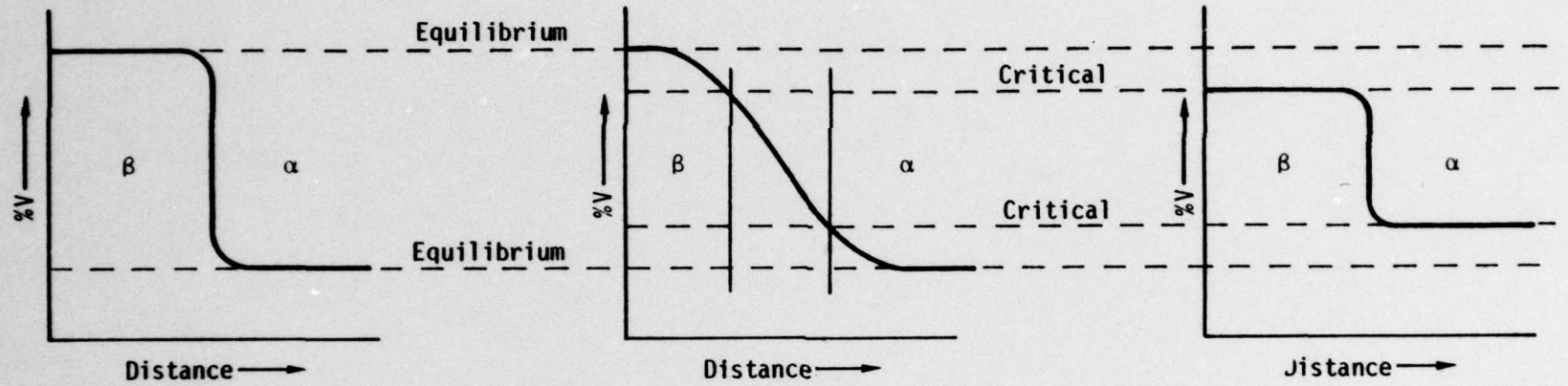

Fig. 13 Schematic description of vanadium concentration gradient in three regions of Figure 3 corresponding to (I) very slow cooling rate, (II) intermediate cooling rate, and (III) rapid cooling rate.